

Open-Loop Tip Accuracy of an MRI-Compatible Active Cannula Robot

D.B. Comber¹, E.J. Barth¹, R.J. Webster III¹, J.S. Neimat²

¹Department of Mechanical Engineering, Vanderbilt University

²Department of Neurological Surgery, Vanderbilt University Medical Center
eric.j.barth@vanderbilt.edu

INTRODUCTION

Magnetic resonance imaging (MRI) is increasingly used intraoperatively, because it provides excellent soft tissue distinction and on-the-fly adjustment to imaging slice orientation without exposing clinician or patient to radiation. For neurosurgical procedures, intraoperative MRI holds significant advantages over traditional stereotactic methods (e.g. compensation for brain shift), and has thereby led to much research toward minimally invasive treatments of brain tumors, epilepsy, and other neurological disorders. Because the tight confines of MRI scanners limit clinician access to the patient, an MRI-compatible robot is potentially useful for many procedures and additionally offers the clinician increased accuracy and degrees of freedom within the minimally invasive context.

Affecting 0.5 to 1.0% of the global population, epilepsy is a neurological disorder for which surgery has been reported superior to prolonged pharmacotherapy, yet only a small fraction of potential surgical candidates receive treatment [1]. Minimally invasive alternatives to conventional resection of seizure foci could side-step the potential morbidity and lengthy recovery associated with open brain surgery thereby making surgical treatment and cure available to a greater number of patients with less risk. Interstitial laser ablation of seizure foci has been clinically demonstrated using MRI to guide ablator placement and MR thermometry for thermal dosimetry [2]. This procedure currently requires multiple patient transfers between MRI scanner and operating room meaning that introducing an MRI-compatible robot could streamline surgical workflow. An alternative real-time MRI approach is high intensity focused ultrasound (HIFU), yet intracranial targets can be difficult to effectively treat due to high reflection and absorption of the ultrasound energy by the skull [3].

This paper reports a pneumatically-actuated active cannula robot designed for MRI-guided ablation of epileptogenic foci. An active cannula is a continuum robot consisting of concentric, superelastic nitinol tubes with pre-curved sections. Complex trajectories are realized by translation and rotation of the cannula tubes with respect to one another.

MATERIALS AND METHODS

Since hippocampal sclerosis is present in a majority of epilepsy cases, the hippocampus was selected as the target region for thermal ablation, and an occipital trajectory was deemed optimal for maximizing coverage

through a single needle insertion. Following this trajectory and performing the ablation can be accomplished with five degrees of freedom: two translations and one rotation for the active cannula, and one additional translation and rotation for the ablator. Inclusion of rotation for the ablator provides the option of using an acoustic ablator with radially sectored transducers to direct the ablative energy [4].

To manipulate the active cannula and ablator, a robotic platform was designed and built, as shown in Fig. 1. For actuators, pneumatic piston-cylinders with fail-safe rod locks were selected instead of piezoelectric motors, as standard piezoelectric motor drives degrade image quality unless powered down during imaging [5]. Furthermore, pneumatic actuators are quieter than piezoelectrics, pose fewer contamination risks than hydraulics, and can run off a hospital's instrument air facilities. A detailed mechanical design of the robot is reported in [6].

A nonlinear, model-based controller was developed for precision position tracking of the actuators [6]. The electronics dedicated to controlling one actuator are: one 5-port/4-way proportional spool valve, two pressure transducers, one optical encoder for position feedback, and one 5-port/2-way valve for rod lock control. Long pneumatic tubing (3 meters) and shielded cables connect the actuators and optical encoders on the robot to the remotely located valves, pressure transducers and system electronics. The controller was implemented in MATLAB Simulink with xPC target. A supply pressure of 687 kPa was used, providing actuator forces on the order of 40 N.

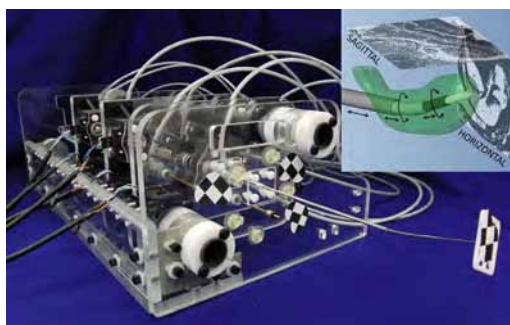


Fig. 1 Photograph of active cannula robot. Inset shows CAD model of cannula and ablator inside hippocampus.

Three tubes were selected for the active cannula and a simulated ablator. Their dimensions are presented in Table 1. The active cannula consists of a stiff, straight outer tube and inner, pre-curved nitinol tube. The outer tube only translates and inner tube both translates and

rotates, as shown in Fig. 1 inset. The inner tube was first curved by hand, and the resulting radius of curvature was estimated using a digital image of the tube.

Table 1 Dimensions of active cannula and simulated ablator tubes

Tube 1 outer diameter	3.18 mm
Tube 1 inner diameter	2.36 mm
Tube 2 outer diameter	1.65 mm
Tube 2 inner diameter	1.35 mm
Tube 2 radius of curvature	132.2 mm
Tube 2 arc length of curved portion	52.0 mm
Simulated ablator outer diameter	1.18 mm

The simulated ablator is a superelastic nitinol tube of outer diameter 1.18 mm. This is slightly smaller than existing MRI-compatible laser ablaters [2], but the rotational mechanism of the robot readily accepts larger tube diameters using an interchangeable collet design.

Prior to in-scanner experiments, an initial benchtop assessment of cannula tip accuracy was needed. Thus, tip position measurements were acquired for 28 robot poses using an optical tracking system, the Micron-Tracker 3 by Claron Technologies (XB3-BW-H3-60). Three optical markers were affixed to the robot front plate. Manufactured from acrylic using a laser cutter, the plate includes pin-sized holes to assist in placing the markers at precisely known positions. Five multi-modality fiducial markers were similarly added for registration with MRI images. An optical marker was fixed to the cannula tip for bench testing with the optical tracker; it will be removed for in-scanner experiments.

Image registration from optical tracker to robot was achieved using point-based registration of the markers on the robot's front plate. Then, for each robot pose, the expected cannula tip position was determined from the robot's forward kinematics. The resulting model-based poses of the robot are illustrated in Fig. 2. Tip error was taken as the difference between measured tip position and tip position expected from the cannula model.

RESULTS

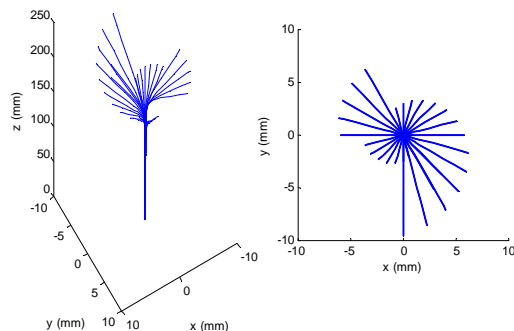


Fig. 2 Model-based poses of the active cannula robot: 3D view (left) and view along the needle guide axis (right).

The mean and maximum tip errors for the 28 cannula poses were 1.18 mm and 2.40 mm, respectively. The fiducial registration error was 0.278 mm, and steady-state errors of the base joints were on the order of 0.050 mm (translations) and 0.5 degrees (rotations).

DISCUSSION

Observing that the registration error and base joint tracking errors are 1 to 2 orders of magnitude below the cannula tip errors, it is reasonable to assume the majority of tip error is due to other sources. One likely cause is inaccuracy in the initial mounting of the cannula tubes; this was done by hand using a ruler and pen. Maximum tip error occurred when the precurved tube was at maximum extension. This error likely arose from the fact that the curvature preset into the curved tube may not have been perfectly circular. The shape setting could be improved by use of a high-precision jig and oven to more precisely set the circular curve.

Nonetheless, the presently observed tip errors are quite small and approach the voxel size for MRI scanners (about $1 \times 1 \times 1 \text{ mm}^3$), and importantly we also note that real-time imaging will be available so that an image-based control loop can be closed on tip position during cannula insertion. Thus, the overall accuracy of tip placement is not limited to the robot's free-space open loop tip accuracy, which is what is reported in this paper. Furthermore, we tested for MRI-compatibility in a Philips 3T Achieva scanner, and the robot displayed no measurable effect on the signal-to-noise ratio of an fBIRN phantom. Image distortion tests with an ADNI phantom indicate a maximum distortion of 1.3 mm.

These results demonstrate that MRI-guided pneumatic actuation is a promising solution for the minimally invasive treatment of epilepsy and of other intracranial diseases that either require or can benefit from MR imaging and thermometry. Future work includes integration of the robotic platform with the MRI scanner. Scanner experiments will focus on providing real-time feedback of tip location as well as using MR thermometry for real-time thermal dosimetry.

REFERENCES

- [1] Engel, J Jr. et al, 2003. "Practice Parameter: Temporal Lobe and Localized Neocortical Resections for Epilepsy," *Epilepsia*, 44(6):741-751.
- [2] Curry, DJ et al, 2012. "MR-Guided Stereotactic Ablation of Epileptogenic Foci in Children," *Epilepsy and Behavior*, 24(4):408-414.
- [3] Basak, A et al, 2012. "Implantable Ultrasonic Dual Functional Assembly for Detection and Treatment of Anomalous Growth," *IEEE Int Conf EMBS*, San Diego, 170-173.
- [4] Kinsey, AM et al, 2008. "Transurethral ultrasound applicators with dynamic multi-sector control for prostate therapy: In vivo evaluation under MR guidance," *J Med Phys*, 35(5):2081-2093.
- [5] Su, H et al, 2011. "High-field MRI-Compatible Needle Placement Robots for Prostate Interventions: Pneumatic and Piezoelectric Approaches," *Advances in Robotics and Virtual Reality*, T Gulrez & A Hassanien, eds, Springer-Verlag, Chap 1.
- [6] Comber, DB et al, 2012. "Sliding Mode Control of an MRI-Compatible Pneumatically Actuated Robot," *Bath/ASME Symp Fluid Power & Motion Control*, DN Johnston and AR Plummer, eds, Centre for Power Transmission & Motion Control, University of Bath, UK, 283-293.